PCCP

RSC Publishing

PAPER

View Article Online
View Journal | View Issue

Cite this: *Phys. Chem. Chem. Phys.*, 2013, **15**, 16634

Effects of cholesterol on membrane molecular dynamics studied by fast field cycling NMR relaxometry

Chu-Jung Hsieh,[a] Yu-Wen Chen[a] and Dennis W. Hwang*[ab]

Received 23rd April 2013,
Accepted 31st July 2013

DOI: 10.1039/c3cp51739j

www.rsc.org/pccp

Biological membranes are complex structures composed of various lipids and proteins. Different membrane compositions affect viscoelastic and hydrodynamic properties of membranes, which are critical to their functions. Lipid bilayer vesicles inserted by cholesterol not only enhance membrane surface motional behavior but also strengthen vesicle stability. Cholesterol-rich vesicles are similar to cell membranes in structure and composition. Therefore, cholesterol-rich vesicles can represent a typical model for studying membrane dynamics and functions. In this study, nuclear magnetic relaxation dispersion was used to investigate the detailed molecular dynamics of membrane differences between vesicles and cholesterol vesicles in the temperature range of 278–298 K. Vesicles of two different sizes were prepared. The effect of cholesterol mainly affected the order fluctuation of membranes and the diffusional motion of lipid molecules. In addition, phase variations were also observed in liposomes that contained cholesterol from analyses of the distances between lipid molecules.

Introduction

Biomembranes, mostly composed of phospholipid molecules and proteins, form an interface to separate intracellular and extracellular space, wherein the phospholipid has a hydrophilic head and takes the lipid bilayer shape. The motion of the phospholipid molecules is affected not only by the elasticity of the lipid bilayer but also by the special function of the membrane, *e.g.*, the permeability of the membrane and the interaction with the surrounding proteins. Thus, the stability of the lipid bilayer is related to the composition and structure of the membranes, temperature range, and degree of hydration.

Singer and Nicholson proposed the fluid-mosaic model of biomembranes to address the importance of the study of phospholipid molecular dynamics.[1] This model implies that biomembranes are in a liquid crystal phase when phospholipid molecules form the lipid bilayer structure. In addition, the membrane structure is subjected to changes in the composition of proteins outside and inside the membrane, which cause lipid bilayers to have different chemical compositions in the inner and outer hydrophilic surfaces. Hence, the properties of membranes can also be used to determine the protein location on the membrane by investigating the specific binding of phospholipid molecules. Moreover, the surface charge of the membrane also affects interactions between the membranes, which may give rise to aggregation and fusion.[2]

Cholesterol plays an interesting role in biomembranes and it is very efficient in altering the biophysical properties of membranes, including their lateral compressibility and permeability to solutes.[3,4] It differs from the other membrane lipid classes, and, in principle, consists of hydrocarbons in the form of a steroid ring structure. Cholesterol appears to have evolved to fill the spaces among the acyl chains in lipid bilayers.[5] It also influences the lateral organization of membrane constituents, resulting in lipid cluster formation and so-called ''rafts.'' Interactions between cholesterol and phospholipids give rise to the changes in membrane properties.[6–9] The cholesterol molecule may form hydrogen bonds with lipid polar groups, including phosphate groups and carbonyls.[10,11]

A wide range of experimental methods have been used to study the detailed effects of cholesterol on the lipid dynamics of membranes. The most commonly used method is nuclear magnetic resonance (NMR) because it is sensitive to dynamics over a very broad time scale.[12–21] In our study, nuclear magnetic relaxation dispersion (NMRD) was used to investigate the detailed molecular dynamics of membranes. By analyzing different molecular motions, the role of the cholesterol molecules in the liposome can be understood clearly. In addition, investigation of different sizes of liposomes at various temperatures allows the mutual effects of size and cholesterol on lipid molecular motion to be distinguished.

[a] *Department of Chemistry and Biochemistry, National Chung Cheng University, No. 168, Sec. 1, University Rd., Min-Hsiung Township Chiayi, 621, Taiwan. E-mail: chedwh@ccu.edu.tw*

[b] *Center for Nano Bio-detection, AIM-HI, National Chung Cheng University, No. 168, Sec. 1, University Rd., Min-Hsiung Township Chiayi, 621, Taiwan*

Experimental section

Sample preparation

Phosphatidyl-choline (PC) represents the head group of lipid. PC has high abundance in biological systems and it is also the most important component in biomembranes. Therefore, 1-palmitoyl-2-oleoyl-phosphatidylcholine (POPC) and POPC/cholesterol liposome suspensions were prepared. Since the NMRD measurements usually take a few hours, the stability of vesicles is crucial to the experiments. Liposomes with the diameters of 100 and 200 nm were prepared because they are stable enough and also big enough to mimic the larger curvature in cellular membranes. The percentage of cholesterol prepared in this study was based on the composition of the cellular membrane, which consists of approximately 30% fat and 20% cholesterol. Therefore, we chose 10% and 30% cholesterol dispersions to investigate its effect on molecular motions of lipids.

For the sample preparation, POPC ($\sim$0.091 g, Avanti Polar Lipids) and cholesterol (10 and 30 mol%, Sigma) were dispersed in adequate ethyl alcohol (Shimakyu's Pure Chemicals) and then sonicated for several minutes until the lipid dissolved. The solvent was removed by rotary evaporation for 20 min. Liposomes were prepared by hydrating the mixtures in 2 mL deuterium oxide (0.06 M lipid), and the suspension was subjected to three shaking/heating cycles to ensure homogeneity. Following hydration, the liposome solutions were kept in warm water (40 °C) and then passed through cellulose acetate membrane filters with pore sizes of 100 and 200 nm (Advantec, Japan).

The liposome sizes were measured using dynamic light scattering (Malvern Instrument). To investigate the effect of cholesterol on liposomes, six samples, denoted by letters A to F, were prepared; the details are listed in Table 1.

NMR measurements

Measurements of the spin–lattice relaxation time were performed using a SPINMASTER FFC-2000 (Stelar s.l.r.) fast field cycling NMR relaxometer over a continuum of magnetic fields from 2.35×10^{-4} to 0.94 T (corresponding to a proton Larmor frequency range of 0.01–40 MHz) and required the use of classical saturation-recovery experimental NMR techniques. The dead time of the spectrometer was $\sim$10 μs. The free induction decay was sampled with 1000 points, after the front edge of the 90° pulse with a duration of 12 μs. In each case, temperature was controlled with a VTC90 temperature controller over the temperature range of 278–298 K.

Table 1 Sample description

Name	Sample description	Diameter (nm) (at 298 K)
A	Pure liposome (small size)	137 ± 8
B	10 mol% cholesterol-containing liposome (small size)	165 ± 14
C	30 mol% cholesterol-containing liposome (small size)	170 ± 3
D	Pure liposome (large size)	248 ± 13
E	10 mol% cholesterol-containing liposome (large size)	257 ± 32
F	30 mol% cholesterol-containing liposome (large size)	353 ± 41

Theory and simulation

To further investigate the molecular dynamics from NMRD data, we used most of the components of the model developed by Meledandri *et al.*[15,16] The molecular motion can be divided into four parts: order fluctuation (OF) of the membrane, diffusional motion (D) of lipid molecules, rotational motion (R) of vesicles, and fast motion (FM). The total T_1 relaxation is given by,

$$R_1 = 1/T_1 = A_{OF}J_{OF}(\omega) + A_D J_D(\omega) + A_R J_R(\omega) + R_{FM} \quad (1)$$

where A is a prefactor of each motion, and J presents the spectral density of each motion mode. Because only dipolar interactions are considered, the prefactor is defined as $(9/8r^6)\gamma^4(h/2\pi)^2(\mu_0/4\pi)^2$, where r is the distance between phospholipid molecules, γ is the gyromagnetic ratio of a proton, and μ_0 is the vacuum magnetic permeability. The order fluctuation mainly describes the degree of deformation of the whole liposome. The detailed spectral density for order fluctuation is given by[22–24]

$$J_{OF}(\omega) = \frac{k_B T}{2\pi\kappa}\sum_{l=2}^{l_{max}} \frac{l(l+2)(2l+1)\tau_l}{(l^2+l-2)(l^2+l+\sigma)(1+\omega^2\tau_l^2)} \quad (2)$$

and

$$\tau_l = \frac{\eta R_0^3(2l+1)(2l^2+2l-1)}{\kappa l(l+1)(l+2)(l-1)(l^2+l+\sigma)} \quad (3)$$

where κ is the bending elastic modulus, k_B is the Boltzmann constant, T is the temperature, σ is the effective lateral tension, η is the viscosity of the supporting fluid, and $l_{max} \approx \pi R_0/a$, where a is the average distance between neighboring molecules, and R_0 is the average radius of the spherical liposomes.

The diffusion term expresses the surface diffusion of phospholipid molecules and, in accordance with the theory proposed by Halle, the corresponding spectral density can be expressed by[25]

$$J_D(\omega) = \frac{1}{5}\left[\frac{\tau_D}{1+(\omega\tau_D)^2} + \frac{4\tau_D}{1+(2\omega\tau_D)^2}\right] \quad (4)$$

where τ_D is the diffusion correlation time and can be divided into rotational and translational diffusion as $1/\tau_D = 1/\tau_{RD} + 1/\tau_{TD}$; τ_{RD} is the rotational diffusion and is equal to $4\pi\eta R_0^3/3k_BT$. Because the rotational diffusion correlation time can be deduced from the known properties of samples, we mostly focused on the translational diffusion, τ_{TD}, in this study: $\tau_{TD} = R_0^2/6D$, where D is the diffusion coefficient. The major difference from previous work is the rotational motion term.[15,16] In this study, we specified it as the rotational motion of the whole liposome. The spectral densities are similar to eqn (4) but with diffusion correlation time, τ_D, replaced by rotational correlation time, τ_R. The fast motion term in eqn (1) is responsible for motion that is sufficiently fast and has no relaxation variation

in the acquisition field range. According to the motional narrowing limit ($\omega\tau \approx 1$) and the field used in this study ($\omega \leq 40$ MHz), any motion time scale faster than 2.5×10^{-8} s is classified as fast motion.

The field-dependent relaxation curve was fitted by eqn (1). Simulations were performed in MATLAB (MathWorks Inc.). Fitting was optimized by a least-squares method.

Results and discussion

Comparison of NMRD in each sample

The field-dependent relaxivity indicates the motional variation in the liposome. Fig. 1(a)–(c) demonstrate the NMRD of samples A, B, and C, respectively, whose diameters are estimated to be 129–147 nm depending on the cholesterol concentration and temperature. In the temperature range from 278 to 298 K, the field-dependent relaxations show good agreement at low magnetic fields and diverge at high magnetic fields. At high magnetic fields, lower temperature shows faster relaxation. The relaxation behavior also depends on the cholesterol concentration. At low fields, samples containing less cholesterol exhibit slower T_1 relaxation times than those containing more cholesterol, whereas an opposite trend is observed at high fields. In addition, when temperature is varied, the T_1 relaxation times of liposomes with higher cholesterol concentrations are more diverse than those with lower cholesterol concentrations. Moreover, liposomes with lower cholesterol concentrations also exhibit smoother variations at low fields than at higher fields.

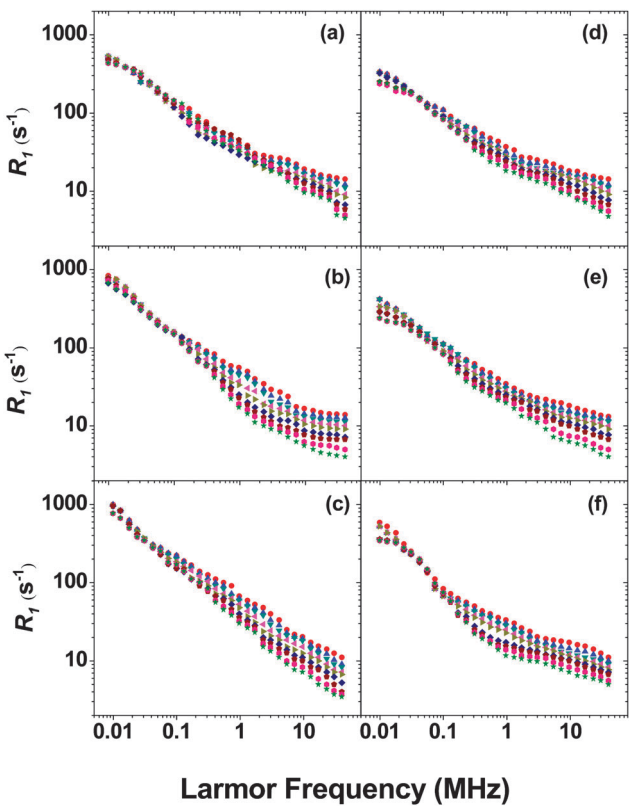

Fig. 1 NMR dispersion of samples (a) A, (b) B, (c) C, (d) D, (e) E, and (f) F. The curves (reading downward) are temperatures of 278 K (●), 281 K (▲), 283 K (▼), 286 K (◀), 288 K (▶), 291 K (◆), 293 K (⬟), 296 K (⬣), and 298 K (★).

The size of a liposome is critical to the membrane dynamics. Therefore, larger liposomes were also investigated. Fig. 1(d)–(f) demonstrate the NMRD of samples D, E, and F, respectively, whose diameters were estimated to be 248–353 nm depending on the cholesterol concentration and temperature. Generally, the relaxivity of larger-sized samples (D, E, and F) was lower than that of smaller-sized samples (A, B, and C) at low fields. Moreover, sample F showed unusual temperature dependency between 288 and 291 K. Nevertheless, similar to smaller-sized samples, T_1 relaxation showed significant temperature dependence at high fields.

Order fluctuation of liposomes

The fitting results are listed in Tables 2–7. Relaxation caused by order fluctuation mainly affects the elasticity, κ, of a liposome. Fig. 2 shows elasticity *versus* the reciprocal of temperature. Generally, higher cholesterol concentrations in liposomes result in greater elasticity. Greater elasticity means more energy is consumed during bending and implies a more rigid structure. Hence, the addition of cholesterol into lipid molecules makes the structures more stable. In addition, the liposome size also affects the membrane elasticity. The elasticity in large liposomes is considerably influenced by the cholesterol concentration, as demonstrated in samples D, E, and F. In contrast, the effect of cholesterol is insignificant in smaller liposomes.

The average distance between lipid molecules determined by analysis of the prefactor A_{OF} can be used to interpret elasticity variation. The distance between lipid molecules was estimated to be $\sim$0.50, 0.52, 0.35, 0.66, 0.66, and 0.31 nm for samples A, B, C, D, E, and F, respectively. Because cholesterol molecules caused lipid molecules to come closer, structures became tightly packed, resulting in difficulty for the membrane to fluctuate. Nevertheless, because the distance between lipid molecules in smaller liposomes, *i.e.*, samples A, B, and C, varied relatively less than that in larger liposomes, the elasticity smoothly changed with increasing cholesterol concentrations. However, the differences between samples A and B and between samples D and E are not substantial (Fig. 2) compared with the differences between samples with higher cholesterol concentrations. These differences result from the fact that the cholesterol molecules first insert into the inner layer of liposomes. When the cholesterol concentration is low, the outer layer of liposomes may still maintain a structure similar to that of a pure liposome.[26]

Translational diffusion of lipid molecules

The diffusional motion of lipid molecules also affects the T_1 relaxation time. Both translational and rotational diffusional motions are involved. The latter is mostly dominated by the solvent viscosity and temperature. Therefore, translational motions are primarily discussed here. Fig. 3 demonstrates the Arrhenius plot of the diffusion coefficients and shows that the diffusion coefficient decreases with increasing cholesterol concentration.

Table 2 Fitting parameters obtained from experimental data for sample A

Temp. (K)	A_{OF} ($\times 10^7$)	κ (J) ($\times 10^{-20}$)	A_D ($\times 10^7$)	D ($m^2\ s^{-1}$) ($\times 10^{-11}$)	A_R ($\times 10^7$)	τ_R (s) ($\times 10^{-6}$)	R_{FM}
278	12 ± 0.5	5.3 ± 0.3	1.5 ± 0.1	1.3 ± 1.1	2.9 ± 0.2	8.0 ± 0.5	20 ± 2.0
281	12 ± 0.5	4.5 ± 0.5	1.5 ± 0.2	1.5 ± 1.2	2.9 ± 0.3	7.5 ± 0.8	19 ± 1.5
283	10 ± 0.3	4.0 ± 0.4	1.5 ± 0.2	1.9 ± 1.5	2.9 ± 0.3	6.0 ± 1.1	14 ± 2.0
286	2.5 ± 0.1	3 ± 1.5	1.6 ± 0.1	2.5 ± 0.4	3 ± 0.2	5 ± 0.5	11 ± 1.5
288	2.5 ± 0.1	2.5 ± 1.2	1.6 ± 0.1	3.1 ± 0.1	3 ± 0.2	4.7 ± 0.6	11 ± 1.0
291	2.5 ± 0.1	2 ± 3.0	1.5 ± 0.1	4 ± 0.1	3 ± 0.1	4 ± 0.2	11 ± 1.0
293	1.0 ± 0.1	1.5 ± 0.2	1.2 ± 0.1	4.8 ± 0.6	3.3 ± 0.1	3.6 ± 0.1	13 ± 2.0
296	5.0 ± 3.0	1.0 ± 0.5	1 ± 0.1	5 ± 0.9	3.2 ± 0.3	3.0 ± 0.5	10.3 ± 2.0
298	6.8 ± 1.1	1.0 ± 0.1	1 ± 0.1	5 ± 0.5	3.2 ± 0.1	2.8 ± 0.2	9.3 ± 1.5

Table 3 Fitting parameters obtained from experimental data for sample B

Temp. (K)	A_{OF} ($\times 10^7$)	κ (J) ($\times 10^{-20}$)	A_D ($\times 10^7$)	D ($m^2\ s^{-1}$) ($\times 10^{-11}$)	A_R ($\times 10^7$)	τ_R (s) ($\times 10^{-6}$)	R_{FM}
278	2.5 ± 0.3	7.8 ± 0.3	8 ± 0.1	1.5 ± 0.1	3.2 ± 0.1	10 ± 0.8	20.5 ± 1.5
281	2.5 ± 0.2	4.7 ± 0.2	8 ± 0.2	1.8 ± 0.1	3 ± 0.1	7.2 ± 0.9	20 ± 0.8
283	4 ± 0.3	3.8 ± 0.4	4.9 ± 0.5	2 ± 0.4	3 ± 0.1	7 ± 0.2	15.2 ± 1.2
286	3.2 ± 0.3	3.5 ± 0.0	5.3 ± 0.1	2.3 ± 0.3	3.1 ± 0.1	6.4 ± 0.1	15 ± 0.2
288	1.0 ± 0.5	3 ± 0.2	5.1 ± 0.3	2.5 ± 0.2	3.3 ± 0.1	5.9 ± 0.1	10.4 ± 0.2
291	2.5 ± 0.1	3 ± 0.2	5 ± 0.1	3 ± 0.0	3 ± 0.1	5.7 ± 0.2	10 ± 0.5
293	2.4 ± 0.3	1.9 ± 0.2	5.2 ± 0.2	3.5 ± 0.2	3 ± 0.1	5.5 ± 1.0	10 ± 0.2
296	2.5 ± 0.1	1.1 ± 0.1	5.1 ± 0.1	3.8 ± 0.4	3 ± 0.1	5.2 ± 0.2	9.8 ± 0.1
298	2.6 ± 0.1	1.1 ± 0.2	5.1 ± 0.1	4 ± 0.3	3 ± 0.0	4.5 ± 0.2	9.4 ± 0.3

Table 4 Fitting parameters obtained from experimental data for sample C

Temp. (K)	A_{OF} ($\times 10^8$)	κ (J) ($\times 10^{-20}$)	A_D ($\times 10^7$)	D ($m^2\ s^{-1}$) ($\times 10^{-11}$)	A_R ($\times 10^7$)	τ_R (s) ($\times 10^{-6}$)	R_{FM}
278	15 ± 2.1	6.0 ± 0.1	33 ± 1.2	0.9 ± 0.1	2.3 ± 0.1	11 ± 0.2	27 ± 1.1
281	9.0 ± 1.5	5.0 ± 0.2	27 ± 1.1	0.9 ± 0.1	2.5 ± 0.0	10 ± 0.3	24 ± 2.1
283	8.0 ± 0.8	4.2 ± 0.2	30 ± 1.1	0.9 ± 0.2	2.2 ± 0.1	10 ± 0.2	25 ± 1.5
286	7.9 ± 0.9	3.9 ± 0.1	33 ± 1.5	0.9 ± 0.1	2.2 ± 0.1	9.3 ± 0.0	23 ± 1.0
288	4.9 ± 0.3	3.6 ± 0.6	31 ± 1.0	1.0 ± 0.2	2.3 ± 0.1	9.0 ± 0.1	18 ± 1.0
291	2.5 ± 0.1	3.2 ± 0.5	10 ± 0.4	1.7 ± 0.1	3 ± 0.1	8.3 ± 0.1	20 ± 2.0
293	1.1 ± 0.2	2.9 ± 0.2	21 ± 0.5	2.0 ± 0.1	2.7 ± 0.1	7.8 ± 0.1	17 ± 3.0
296	2.5 ± 0.1	2.5 ± 1.2	5 ± 0.1	2.4 ± 0.9	3 ± 0.1	7.7 ± 0.1	10 ± 0.1
298	2.5 ± 0.1	2.4 ± 0.8	5 ± 0.1	2.6 ± 2.1	3 ± 0.1	7.2 ± 0.1	10 ± 0.5

Table 5 Fitting parameters obtained from experimental data for sample D

Temp. (K)	A_{OF} ($\times 10^6$)	κ (J) ($\times 10^{-20}$)	A_D ($\times 10^6$)	D ($m^2\ s^{-1}$) ($\times 10^{-11}$)	A_R ($\times 10^7$)	τ_R (s) ($\times 10^{-6}$)	R_{FM}
278	5 ± 5.0	4 ± 0.8	5 ± 0.3	4.0 ± 1.0	2 ± 0.3	5.5 ± 0.2	20 ± 1.5
281	5 ± 4.5	3.5 ± 2.0	5 ± 0.4	4.2 ± 0.7	2 ± 0.2	5.3 ± 0.3	17 ± 1.2
283	8 ± 5.5	3 ± 1.5	5 ± 0.4	4.4 ± 0.8	2 ± 0.4	5.2 ± 0.2	17 ± 0.5
286	9 ± 3.5	2.5 ± 2.0	5.2 ± 0.5	4.5 ± 1.2	1.8 ± 0.3	5 ± 0.0	16 ± 0.0
288	8 ± 4.0	2.3 ± 1.2	5 ± 0.3	4.5 ± 0.4	1.8 ± 0.1	4.7 ± 0.2	15 ± 0.1
291	8 ± 5.0	1.8 ± 2.0	5 ± 0.4	4.9 ± 1.5	1.9 ± 0.0	4.6 ± 0.1	10 ± 1.5
293	9 ± 4.0	1.5 ± 0.0	5 ± 0.3	4.9 ± 0.7	0.5 ± 0.7	3.8 ± 0.1	10 ± 1.0
296	8.5 ± 1.2	1.3 ± 0.5	5.5 ± 0.2	5.1 ± 0.2	2 ± 0.2	2.8 ± 0.1	6.5 ± 0.5
298	8.5 ± 2.6	1.2 ± 0.2	5.5 ± 0.5	5.2 ± 1.2	2 ± 0.2	2.8 ± 0.2	4.5 ± 2.0

Table 6 Fitting parameters obtained from experimental data for sample E

Temp. (K)	A_{OF} ($\times 10^6$)	κ (J) ($\times 10^{-20}$)	A_D ($\times 10^6$)	D ($m^2\ s^{-1}$) ($\times 10^{-11}$)	A_R ($\times 10^7$)	τ_R (s) ($\times 10^{-6}$)	R_{FM}
278	5.0 ± 0.1	5.5 ± 1.5	6.0 ± 1.5	1.8 ± 0.3	2.0 ± 0.0	6.5 ± 0.1	20.6 ± 0.1
281	8.0 ± 0.2	4.5 ± 2.0	5.9 ± 3.5	2.4 ± 1.2	2.1 ± 0.1	6 ± 0.2	18.1 ± 0.5
283	8.9 ± 1.5	4.0 ± 1.0	5.9 ± 1.5	2.8 ± 0.4	2.1 ± 0.1	5.5 ± 0.1	17 ± 0.1
286	8.3 ± 2.0	3.8 ± 1.1	5.4 ± 1.2	3.5 ± 0.5	2.0 ± 0.1	5.0 ± 0.0	14.9 ± 0.0
288	8.1 ± 1.5	3.0 ± 0.1	5.0 ± 1.3	3.7 ± 0.2	2.0 ± 0.1	4.5 ± 0.2	13.5 ± 0.5
291	8.5 ± 1.8	2.9 ± 2.5	5.4 ± 2.5	4.1 ± 1.1	2.0 ± 0.2	3.8 ± 0.1	10.5 ± 2.5
293	9.0 ± 5.1	2.8 ± 0.5	5.0 ± 1.1	5.0 ± 0.4	2.1 ± 0.1	3.5 ± 0.1	9.2 ± 1.1
296	9.0 ± 4.2	2.8 ± 0.0	5.0 ± 0.8	5.0 ± 0.2	2.3 ± 0.0	2.6 ± 0.2	5.0 ± 0.8
298	8.2 ± 0.9	2.8 ± 0.1	5.0 ± 2.5	5.0 ± 0.7	2.3 ± 0.2	2.5 ± 0.2	4.8 ± 0.1

Table 7 Fitting parameters obtained from experimental data for sample F

Temp. (K)	A_{OF} ($\times 10^8$)	κ (J) ($\times 10^{-20}$)	A_D ($\times 10^7$)	D ($m^2\ s^{-1}$) ($\times 10^{-11}$)	A_R ($\times 10^6$)	τ_R (s) ($\times 10^{-6}$)	R_{FM}
278	5 ± 0.1	10 ± 0.5	100 ± 1.2	0.8 ± 0.3	13 ± 0.2	11 ± 0.3	16 ± 1.5
281	5 ± 0.1	9.7 ± 0.6	100 ± 1.2	0.9 ± 0.4	16 ± 0.2	10 ± 0.5	15 ± 2.1
283	10 ± 2.0	8.3 ± 0.3	50 ± 1.2	1.0 ± 0.5	9 ± 0.5	9.3 ± 0.3	12 ± 1.2
286	10 ± 1.0	7.5 ± 0.1	50 ± 1.1	1.3 ± 0.1	5.5 ± 0.1	8.8 ± 0.1	9 ± 0.1
288	7 ± 0.1	7.5 ± 0.2	50 ± 0.2	1.9 ± 0.3	5.5 ± 0.1	8.5 ± 0.6	9 ± 1.2
291	9 ± 0.1	7 ± 0.1	1.5 ± 0.1	2.2 ± 0.1	5.5 ± 0.1	7.2 ± 0.5	8.5 ± 1.5
293	9 ± 0.1	7 ± 0.0	1.5 ± 0.1	2.4 ± 0.6	5.5 ± 0.1	6.3 ± 0.2	6 ± 0.2
296	9 ± 0.1	7 ± 0.1	1.5 ± 0.1	2.8 ± 0.8	5.5 ± 0.1	5.7 ± 0.2	5 ± 0.0
298	9 ± 0.1	6.8 ± 0.1	1.5 ± 0.1	3 ± 0.2	5.5 ± 0.1	5 ± 0.1	5 ± 0.0

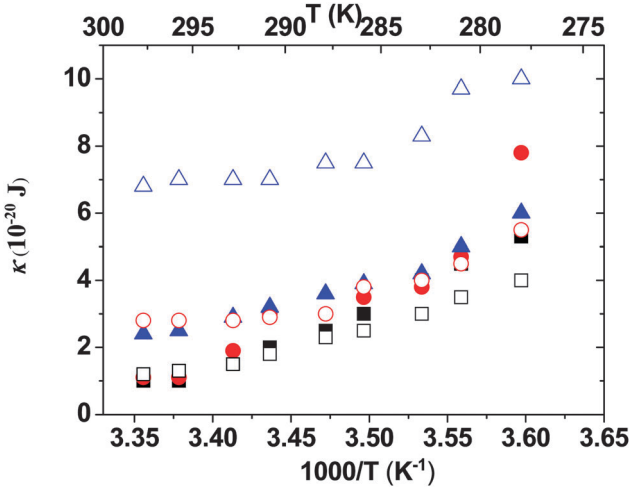

Fig. 2 Elasticity *versus* the reciprocal of temperature in samples A (■), B (●), C (▲), D (□), E (○), and F (△).

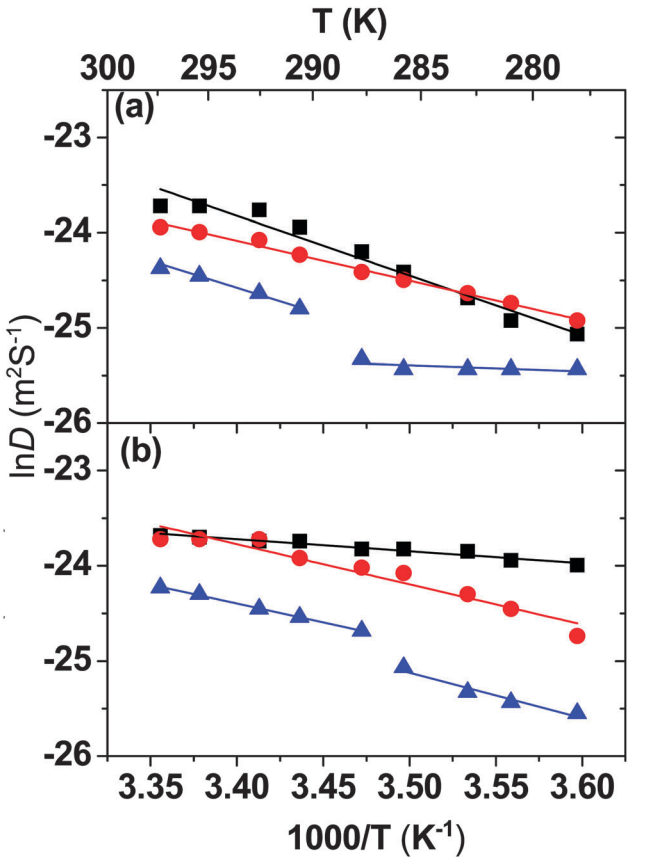

Fig. 3 Arrhenius plot of the diffusion coefficient in (a) in samples A (■), B (●), and C (▲) and in (b) samples D (■), E (●), and F (▲).

However, the effect of size on the translational motion of the lipid was not significant (Fig. 3).

Increased cholesterol concentration caused interesting non-linear temperature dependence in both size samples. Two discontinuous slopes were observed below and above 288 K. The slope difference was significant in sample C (Fig. 3(a)), whereas it only showed a discontinuity in sample F (Fig. 3(b)). However, the distance between lipid molecules evaluated from prefactors of diffusional motion, A_D, showed a significant distance variation in samples C and F around 288 K (Fig. 4). A liposome that consists of POPC is believed to be in a mixed state of liquid-ordered and liquid-disordered phases when cholesterol is added.[7,27] When temperature varies, it may change the ratio of these two phases. This variation may primarily result in the distance change, *i.e.*, the entropy effect, and may only weakly affect the interaction between lipid molecules. Consequently, the slope in Fig. 4 shows a discontinuity but a similar slope. Fig. 4 also displays that the addition of cholesterol molecules forces lipid molecules to come closer. As a result, translational diffusion of lipid molecules becomes more difficult.

Rotational correlation time of liposomes

The rotational correlation time, τ_R, mentioned here corresponds to the rotational motion of the whole liposome, and the values obtained from fitting agree with the time scale of the rotational time of nanometer-sized particles. According to Stokes' law, the relationship between rotational correlation time and viscosity is given by

$$\tau_R = \frac{4\pi R_0^3 \eta}{3kT} \quad (5)$$

where R_0 is the radius of the particle, and η is the viscosity. Because $\eta \propto e^{E_a/kT}$ in a liquid, eqn (5) can be rewritten as

$$\tau_R \propto \frac{4\pi R_0^3 e^{E_a/kT}}{3kT} \quad (6)$$

Fig. 5 illustrates the fitting rotational correlation time, τ_R, divided by $4\pi R_0^3$ plotted against inversed temperature fitted by

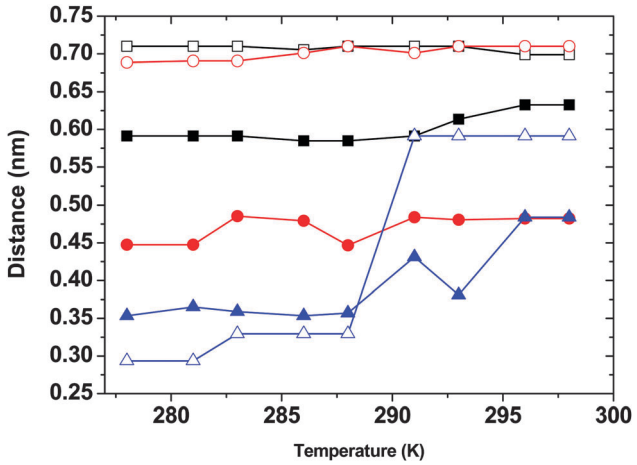

Fig. 4 Distance between lipid molecules evaluated from the prefactor, A_D, *versus* temperature in samples A (■), B (●), C (▲), D (□), E (○), and F (△).

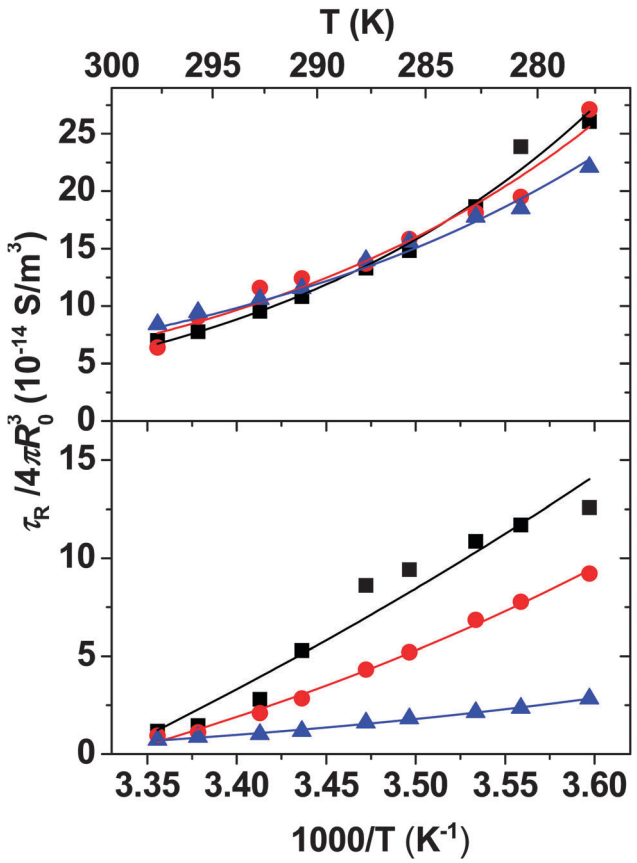

Fig. 5 Plot of rotational correlation time, τ_R, divided by $4\pi R^3$ plotted against inversed temperature in (a) samples A (■), B (●), and C (▲) and (b) samples D (■), E (●), and F (▲).

eqn (6). The plot shows a good agreement between the experimental data and the fitting curves. The obtained activation energies were 5.6×10^{-20}, 5.8×10^{-20}, 5.7×10^{-20}, 1.2×10^{-20}, 2.7×10^{-20}, and 3.6×10^{-20} J for samples A, B, C, D, E, and F, respectively. Generally, the interaction between liposomes is stronger in small size liposomes. However, in samples A, B, and C, which are small size liposomes, the interaction between the liposomes was similar, whereas it significantly changed for large liposomes, *i.e.*, for samples D, E, and F. Two effects, size and interaction between liposomes, influence the rotational motion of liposomes. Because this interaction occurs over long distances and is weak, its effect on the system would be to slow down rotational motion, which suggests large-sized liposome behavior. The interaction between liposomes changes with the cholesterol concentration.[28] The addition of cholesterol into a lipid bilayer decreases the surface charge and possibly results in the surface binding force between the liposome and the cation in the solution being weakened. As a result, the interaction between liposomes becomes stronger when cholesterol is added.

Conclusion

In this study, NMRD was used to investigate the detailed molecular dynamics of membrane differences between vesicles and cholesterol vesicles in the temperature range of 278–298 K. These findings provide a quantitative explanation to confirm previous work on the stability of cholesterol vesicles. Two different liposome sizes were prepared. Cholesterol mainly affected the order fluctuation of the membrane and the diffusional motion of lipid molecules. In addition, phase variations were also observed in liposomes that contained 30 mol% cholesterol from analyses of the distances between lipid molecules. Moreover, the temperature dependence of the rotational motion of liposomes was affected by the interaction between liposomes. A higher cholesterol concentration caused weaker surface charge and less shielding effect of liposomes. As a result, a stronger repulsive force was found in liposomes that contained a higher cholesterol concentration.

Acknowledgements

This study was supported by the National Science Council of the Republic of China under grant no. NSC 101-2113-M-194-006-MY2. We thank the Instruments Center at National Chung Cheng University (Taiwan) for their excellent technical assistance with the fast field cycling NMR relaxometry.

References

1 S. J. Singer and G. L. Nicolson, *Science*, 1972, **175**, 720–730.
2 D. E. Lee, M. G. Lew and D. J. Woodbury, *Chem. Phys. Lipids*, 2013, **166**, 45–54.
3 P. L. G. Chong, W. W. Zhu and B. Venegas, *Biochim. Biophys. Acta, Biomembr.*, 2009, **1788**, 2–11.
4 C. Dahl and J. Dahl, in *Biology of cholesterol*, ed. Y. PL, CRC Press, USA, 1988, p. 26.
5 C. Tanford, *The hydrophobic effect: formation of micelles and biological membranes*, John Wiley & Sons, USA, 1980.
6 H. Ohvo-Rekila, B. Ramstedt, P. Leppimaki and J. P. Slotte, *Prog. Lipid Res.*, 2002, **41**, 66–97.
7 T. P. W. McMullen, R. N. A. H. Lewis and R. N. McElhaney, *Curr. Opin. Colloid Interface Sci.*, 2004, **8**, 459–468.

8 S. Jo, H. Rui, J. B. Lim, J. B. Klauda and W. Im, *J. Phys. Chem. B*, 2010, **114**, 13342–13348.
9 S. Mondal and C. Mukhopadhyay, *Chem. Phys. Lett.*, 2007, **439**, 166–170.
10 J. R. Silvius, *Biochim. Biophys. Acta, Biomembr.*, 2003, **1610**, 174–183.
11 J. Aittoniemi, P. S. Niemelä, M. T. Hyvönen, M. Karttunen and I. Vattulainen, *Biophys. J.*, 2007, **92**, 1125–1137.
12 S. I. Chan, G W. Feigenso and C. H. A. Seiter, *Nature*, 1971, **231**, 110–112.
13 H. Wennerst, *Chem. Phys. Lett.*, 1973, **18**, 41–44.
14 M. Bloom, E. E. Burnell, M. I. Valic and G. Weeks, *Chem. Phys. Lipids*, 1975, **14**, 107–112.
15 C. J. Meledandri, J. Perlo, E. Farrher, D. F. Brougham and E. Anoardo, *J. Phys. Chem. B*, 2009, **113**, 15532–15540.
16 J. Perlo, C. J. Meledandri, E. Anoardo and D. F. Brougham, *J. Phys. Chem. B*, 2011, **115**, 3444–3451.
17 Q. Saleem, A. Lai, H. H. Morales and P. M. Macdonald, *Chem. Phys. Lipids*, 2012, **165**, 721–730.
18 T. M. Ferreira, F. Coreta-Gomes, O. H. S. Ollila, M. J. Moreno, W. L. C. Vaz and D. Topgaard, *Phys. Chem. Chem. Phys.*, 2013, **15**, 1976–1989.
19 B. Hoff, E. Strandberg, A. S. Ulrich, D. P. Tieleman and C. Posten, *Biophys. J.*, 2005, **88**, 1818–1827.
20 A. Leftin and M. F. Brown, *Biochim. Biophys. Acta, Biomembr.*, 2011, **1808**, 818–839.
21 A. Filippov, G. Oradd and G. Lindblom, *Biophys. J.*, 2003, **84**, 3079–3086.
22 M. Vilfan, G. Althoff, I. Vilfan and G. Kothe, *Phys. Rev. E: Stat. Phys., Plasmas, Fluids, Relat. Interdiscip. Top.*, 2001, **64**, 022902.
23 G. Althoff, D. Frezzato, M. Vilfan, O. Stauch, R. Schubert, I. Vilfan, G. J. Moro and G. Kothe, *J. Phys. Chem. B*, 2002, **106**, 5506–5516.
24 G. Althoff, O. Stauch, M. Vilfan, D. Frezzato, G. J. Moro, P. Hauser, R. Schubert and G. Kothe, *J. Phys. Chem. B*, 2002, **106**, 5517–5526.
25 B. Halle, *J. Chem. Phys.*, 1991, **94**, 3150–3168.
26 F. T. Presti and S. I. Chan, *Biochemistry*, 1982, **21**, 3821–3830.
27 I. V. Ionova, V. A. Livshits and D. Marsh, *Biophys. J.*, 2012, **102**, 1856–1865.
28 D. Z. Liu, W. Y. Chen, L. M. Tasi and S. P. Yang, *Colloids Surf., A*, 2000, **172**, 57–67.

